

Supporting Information

Membrane composition and lipid to protein ratio modulate amyloid kinetics of yeast prion protein

Arnab Bandyopadhyay, Achinta Sannigrahi*, Krishnananda Chattopadhyay*

Structural Biology & Bio-Informatics Division, CSIR-Indian Institute of Chemical Biology,
4, Raja S. C. Mullick Road, Kolkata 700032, India

A

CLUSTAL O(1.2.4) multiple sequence alignment

```

1R5B:A|PDBID|CHAIN|SEQUENCE      SAPAAALKKAAEAAEPATVTEADTLQNEVDQELLLKDMYGKEHVNIIVFIGHVDAGKSTLG      60
SUP35                               -----
1R5B:A|PDBID|CHAIN|SEQUENCE      GNILFLTGIVDKRTMEKIEREAKEAGKESWYLSWALDSTSEEREKGGKTEVVEGRAYFETEH      120
SUP35                               -----MSDS-----NQGNQNYQQYSQNG--NQQGNRRYQGYQAYN---      36
1R5B:A|PDBID|CHAIN|SEQUENCE      RRFSLLDAPGHGKGYVTNMI-----NGASQ--ADIGVLV-----ISARRGEFEAG      162
SUP35                               -----AQA--QPAGGYQNYQGYSGYQQGGYQYNPDAGYQQYNPQGGYQQY-----      91
1R5B:A|PDBID|CHAIN|SEQUENCE      FERGGQTRHAVLARQTGINHLVVVINKMDEPSVQWSEERYKECVDKLSMFLRRVAGYNS      222
SUP35                               -----FNPGGGRGN-----YKNF-----NYNNLQGY--      113
1R5B:A|PDBID|CHAIN|SEQUENCE      KTDVKYNPVSAYTGNVQRVDSVCPWYQGPSLLEYLDSMTHLERKVNAPFI-----M      276
SUP35                               -----QAGFQPSQGMSLNDFQKQKQAAPKPKTKLKLVSSSI      152
1R5B:A|PDBID|CHAIN|SEQUENCE      PIASKYKDLGTILEGK---IEA----GSIKKNSNVLV-----M      307
SUP35                               -----KLANATKKVGTKPAESDKKEEKSAETKEPTKVEEPPVKKEEKPVQTEEKTEEKSEL      212
1R5B:A|PDBID|CHAIN|SEQUENCE      PINQTL-----EVTAIYDEADEEISSICGDQVRLRVGRDSDVQGTGYVL      352
SUP35                               -----PKVEDLKISETHTNNTNANVTSADALIKQEEVDEEVNDGSRALAN*      260
1R5B:A|PDBID|CHAIN|SEQUENCE      TSTKNPVMATTRFIAQIAILELPSILTTGYSVMIHTAVEEVSFAKLLHKLKDKTNRKSK      412
SUP35                               -----
1R5B:A|PDBID|CHAIN|SEQUENCE      KPPMFATKGMKIIAELETQTPVCMERFEDYQYMGFRFLTRDQGTAVAGKVVKILD      467
SUP35                               -----

```

B

CLUSTAL O(1.2.4) multiple sequence alignment

```

1QLX:A|PDBID|CHAIN|SEQUENCE      -----GS-----KKRPKPGGINTGGSRYP-----GQSPGGN-----      27
SUP35                               MSDSNQGNQNYQQYSQNGNQQGNRRYQGYQAYNAQAQAPAGGYQNYQGYSGYQQGGY      60
1QLX:A|PDBID|CHAIN|SEQUENCE      -RYPQGGGGHQPFGGGHGGQ--PHGGHGGPHG--GGWQQ-----PH      65
SUP35                               QQYNPDAGYQQYNPQGGYQQYNPQGGYQQQFNPGGGRGNVKNFNYNLQGYQAGFQPQ      120
1QLX:A|PDBID|CHAIN|SEQUENCE      GGGHGGGGTTHSQWPKPSKPKTNMKHMAGAAAAGAVVGGGLGGYMLGSAMSRPIIHGSDY      125
SUP35                               SQGMSLNDFFQKQKQAAPKPKTKLKLVSSS-----GIKLANA----TKKVGTKP      165
1QLX:A|PDBID|CHAIN|SEQUENCE      EDRIYYRE-----NMHRYPNQV-----YYRPMDE--YSNQNFVHDCVNIITIKQHTV      169
SUP35                               AESDKKEEKSAETKEPTKEPTKVEEPPVKKEEKPVQTEEKTEEKSELPKVEDLKISET-      224
1QLX:A|PDBID|CHAIN|SEQUENCE      TTTTKGENFTETDVKHMERVVEQMCIQYERESQAYYQSGS-----      210
SUP35                               -HNTNANVTSADALIKE-----QEEEVDEEVNDGSRALAN*      260

```

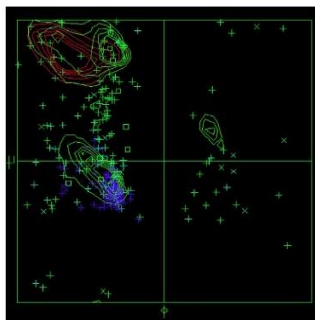
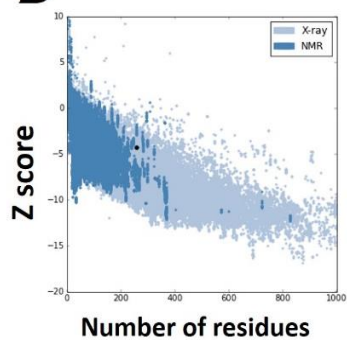
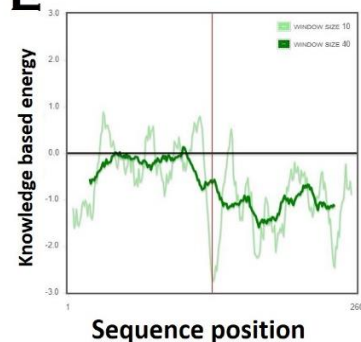
C**D****E**

Figure S1. Validation of the model structure. Multiple sequence alignment of the sequence of prion protein of *S. pompe* (A) and human prion protein (B) with the NM region of yeast prion protein. (C) Ramachandran plot analysis of Sup35 protein. (D) Z score of our model using proSA algorithm. (E) Local model quality predicted by proSA program by plotting energies vs amino acid sequence over the window of 40 residues and 10 residues.

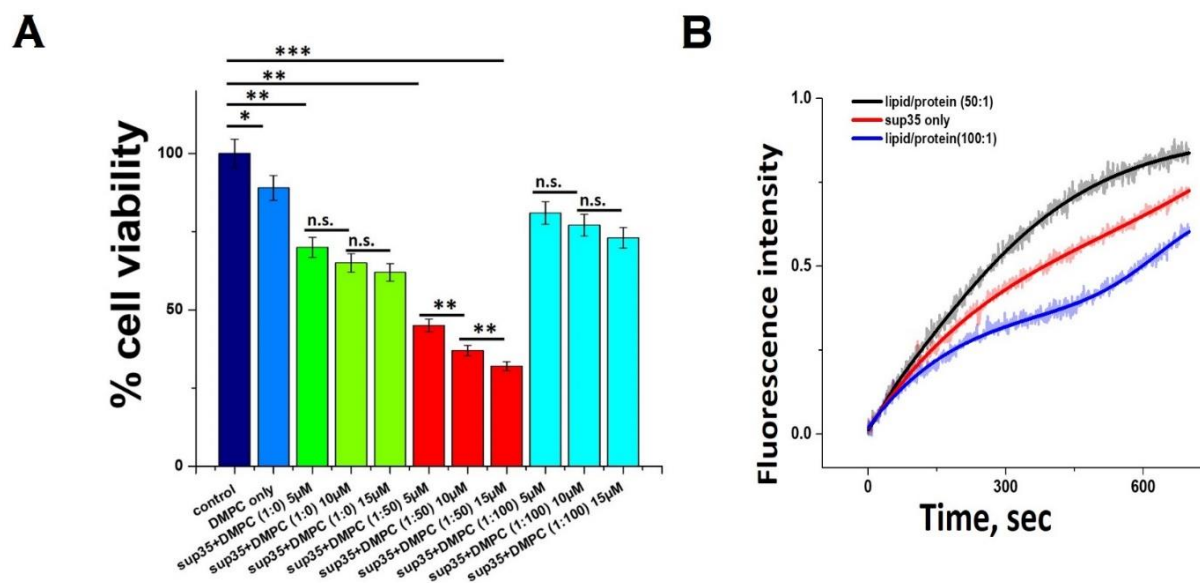


Figure S2. Aggregate-induced differential toxicity of Sup35 in absence and presence of DMPC vesicles. (A) 5µm, 10µm and 15µm concentrations of each aggregate sample were used for the MTT assay to trace the dose dependence on cell viability. Error bar indicates the standard deviation. n.s. stands for non-significant data. For the significant changes- *, P value<0.05; **, P value<0.01; ***, P value<0.001. (B) Calcein release assay using dye entrapped model membrane system in the presence of lipid /protein ratio of 0:1, 50:1 and 100:1.

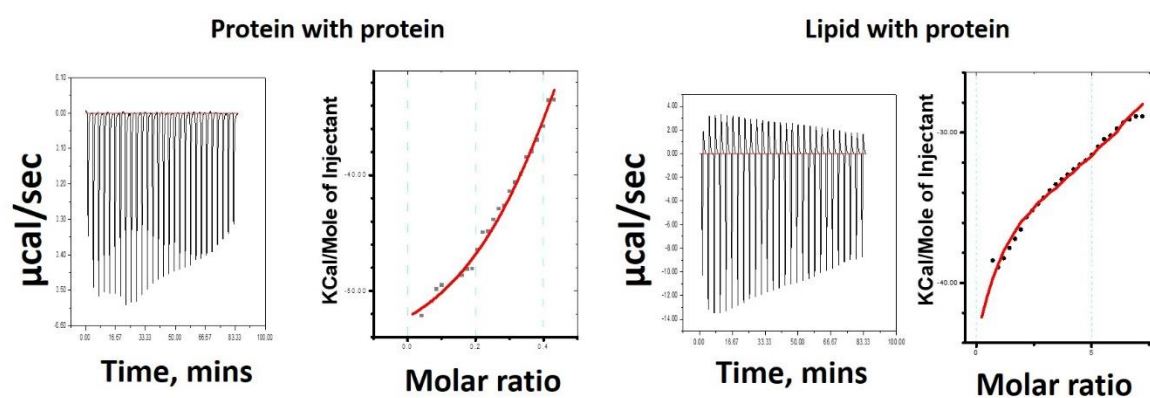


Figure S3. ITC experiments showing binding affinities. The binding isotherm showed the greater binding affinity of Sup35 molecules with itself than its affinity towards DMPC vesicles.

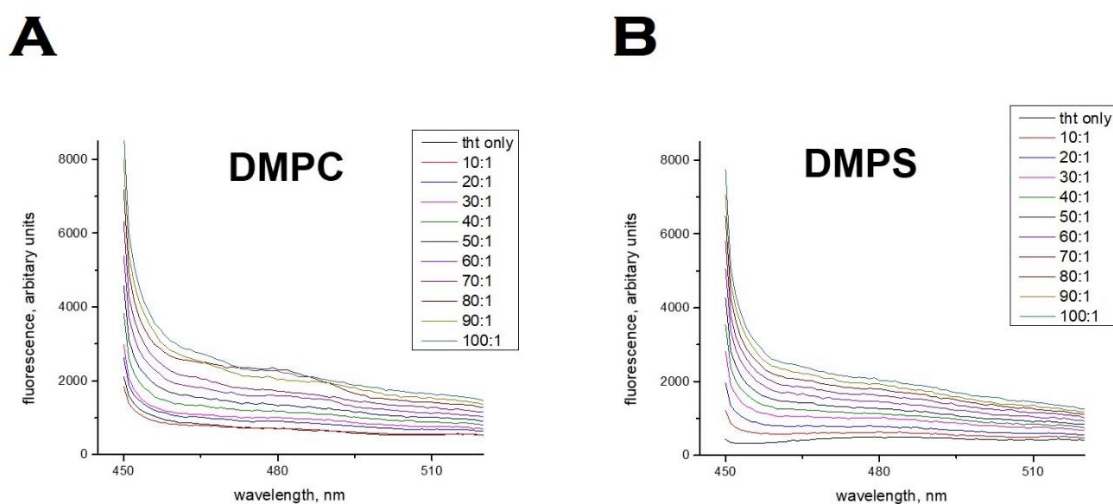


Figure S4. ThT fluorescence showing binding of ThT to lipid vesicles only. (A) with neutral vesicles such as DMPC **(B)** with negatively charged vesicles such as DMPS.

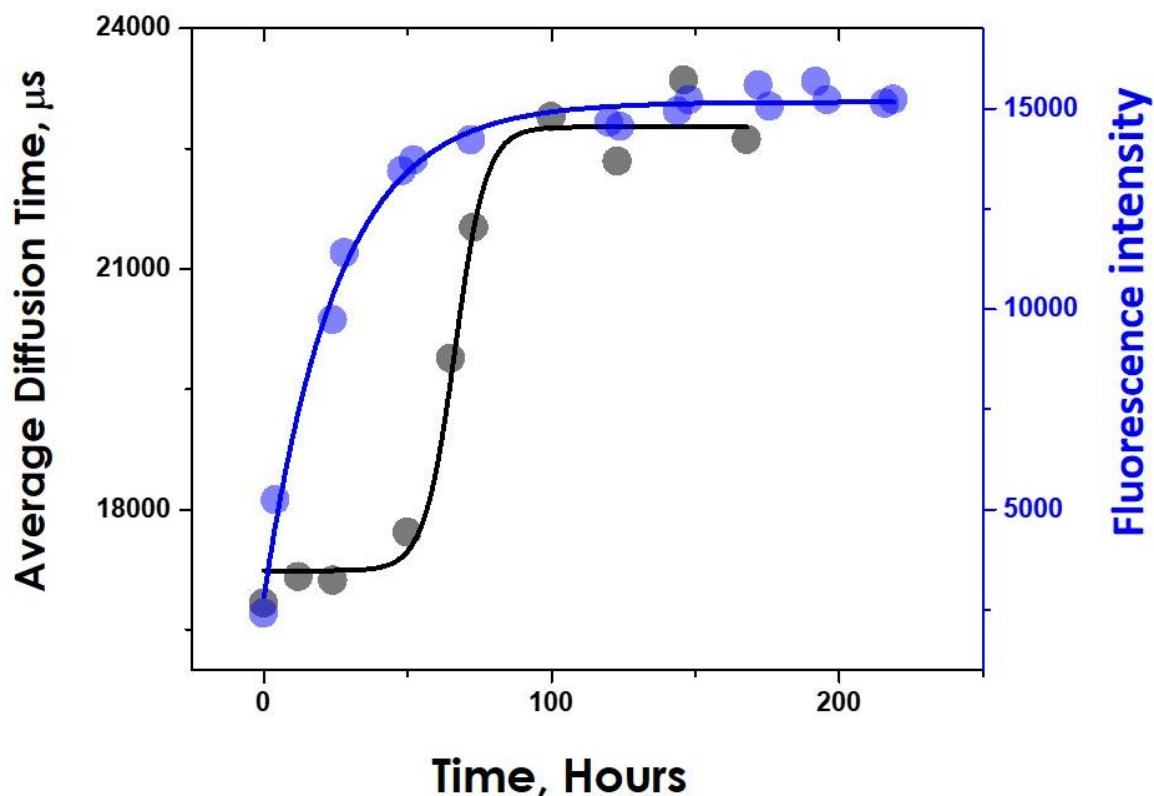


Figure S5. Average diffusion time of aggregates superimposed with ThT fluorescence intensity. ThT monitored aggregation kinetics of Sup35 in the absence of lipid is hyperbolic while the FCS monitored one is sigmoidal.

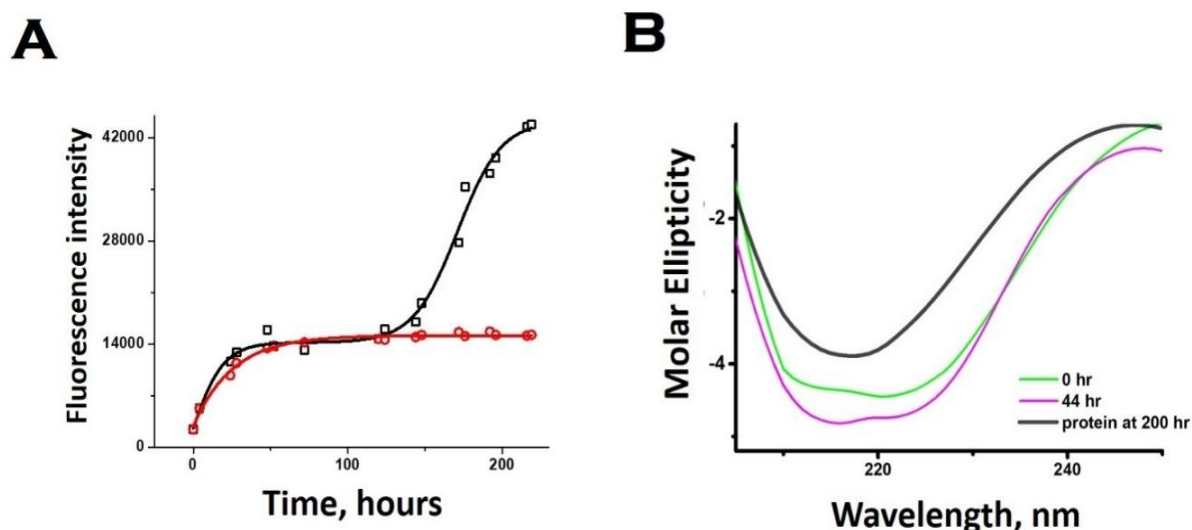


Figure S6. Mechanistic insight on Sup35NM aggregation. (A) Assessment of the aggregation using Thioflavin T fluorescence when membrane environment was introduced to the pre-aggregated Sup35NM. Red line represents the aggregation profile of Sup35NM in the absence of membrane. Black line represents the aggregation profile when membrane was introduced at 130 hours. (B) Far UV-CD experiments of the pre-aggregated species of Sup35NM when incubated with DMPC SUVs maintaining the L/P molar ratio of 100:1 at different time points of incubation.

| Orientation of Proteins in Membranes | | |
|---|------------------------------|---------------------------------------|
| Depth/Hydrophobic Thickness | $\Delta G_{\text{transfer}}$ | Tilt Angle |
| $3.8 \pm 2.0 \text{ \AA}$ | -3.6 kcal/mol | $53. \pm 10.^\circ$ |
| Membrane Embedded Residues (in Hydrocarbon Core) | | |
| Subunits | Tilt | Segments |
| A | 53 | Embedded_residues: 134,137-138,143 |

Figure S7. OPM server results table of membrane binding of Sup35NM.

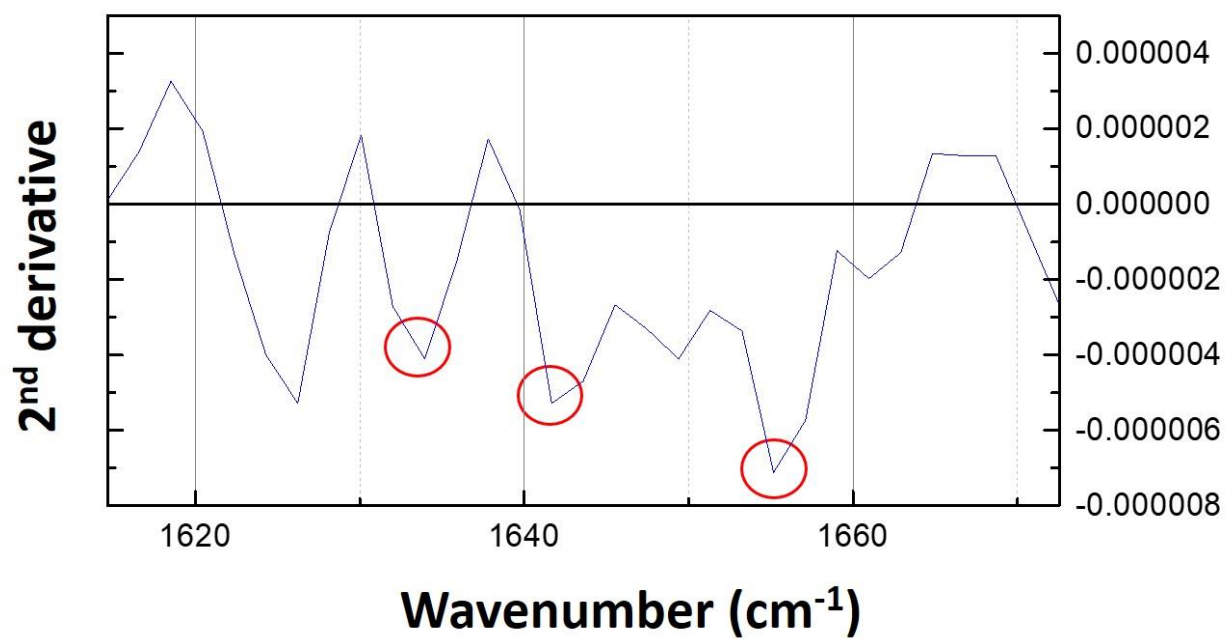


Figure S8. Secondary derivative of the absorbance data of the FTIR spectra of Sup35NM in the absence of lipid. The selected peak regions form the minima of the secondary derivative are marked in red circles.